

Adaptive Algorithm for Chirp-Rate Estimation

Igor Djurović, Cornel Ioana, LJubiša Stanković, and Pu Wang

Abstract— Chirp-rate, as a second derivative of signal phase, is an important feature of nonstationary signals in numerous applications such as radar, sonar, communications, etc. In this paper, an adaptive algorithm for the chirp-rate estimation is proposed. It is based on the confidence intervals rule and the cubic-phase function. The window width is adaptively selected to achieve good trade-off between bias and variance of the chirp-rate estimate. The proposed algorithm is verified by simulations and the results show that it outperforms the standard algorithm with fixed window width.

I. INTRODUCTION

Instantaneous frequency (IF) estimation is a challenging topic in the signal processing [1]. The IF is defined as the first derivative of the signal's instantaneous phase. Time-frequency (TF) representations are main tools for non-parametric IF estimation. The positions of peaks in the TF representation can be used as an IF estimator. There are several sources of errors in this estimator: higher-order derivatives of the signal phase and the noise. For relatively high signal-to-noise ratio (SNR), Stanković and Katkovnik have proposed an IF estimator based on intersection of confidence intervals rule (ICI) that produces results close to the optimal mean squared error (MSE) of the IF estimate, by achieving trade-off between bias and variance [2]-[7].

Sometimes in practice there is a need for an estimation of the second-order derivative of signal phase. Estimation of this parameter, referred to as the chirp-rate, is important in radar systems, for example, focusing of the SAR images [8], [9].

Recently, O'Shea and co-workers have proposed a chirp-rate estimator based on the cubic phase function (CPF) [10]-[14]. It gives

accurate results for a third-order polynomial phase signal. In this paper, we consider non-parametric chirp-rate estimation without the assumption on the polynomial phase structure. To this end, an adaptive algorithm for the chirp-rate estimation is proposed based on the ICI algorithm [15]-[18]. The proposed estimator performs well for moderate noise environments.

The paper is organized as follows. The CPF-based nonparametric chirp-rate estimator is presented in Section II. In Section III asymptotic expressions for the bias and the variance of the nonparametric chirp-rate estimate are provided as a prerequisite for the proposed adaptive algorithm. Full details of the adaptive algorithm based the ICI principle are presented in Section IV. Numerical examples are given in Section V. Conclusions are given in Section VI.

II. CPF-BASED NONPARAMETRIC CHIRP-RATE ESTIMATOR

Consider a signal $f(t) = A \exp(j\phi(t))$. The first derivative of the signal phase, $\omega(t) = \phi'(t)$, is the IF. An important group of the IF estimators is based on TF representations [1], [19], [20]. Consider, for example, the Wigner distribution (WD) in a windowed (pseudo) discrete-time form:

$$WD_h(t, \omega) = \sum_{n=-\infty}^{\infty} w_h(nT)$$

$$\times f(t + nT)f^*(t - nT) \exp(-j2\omega nT), \quad (1)$$

where T is the sampling interval and $w_h(nT)$ is the window function of the width h , $w_h(t) \neq 0$ for $|t| \leq h/2$. The IF can be estimated from locations of peaks in the WD as:

$$\hat{\omega}_h(t) = \arg \max_{\omega} WD_h(t, \omega). \quad (2)$$

A close look at the phase of the local auto-correlation $f(t+nT)f^*(t-nT)$ by means of Taylor expansions is:

$$\begin{aligned}\Phi(t, nT) &= \phi(t+nT) - \phi(t-nT) \\ &\approx 2\phi'(t)(nT) + \phi^{(3)}(t)\frac{(nT)^3}{3} \\ &\quad + \phi^{(5)}(t)\frac{2(nT)^5}{5!} + \dots\end{aligned}\quad (3)$$

where $\phi^{(k)}(t)$, is defined as the k -th derivative of the phase. When higher-order phase derivatives are equal to 0, the WD is ideally concentrated along the IF, i.e., it achieves maximum along the IF line $\omega(t) = \phi'(t)$. Therefore, the IF can be calculated as

$$\phi'(t) \approx \frac{\phi(t+nT) - \phi(t-nT)}{2(nT)}, \quad (4)$$

by ignoring higher-order derivatives.

Estimation of the higher-order phase terms is also very important, for example, in radar signal processing (proper estimation of higher-order phase terms can be helpful in focusing of radar images [21]-[29]). Commonly, higher-order non-linearity exists in the estimate. The non-linearity causes performance degradation of the IF estimate. For example, it reduces the SNR threshold of the method applicability [23].

Analogy to the above observations on the IF estimation, the chirp-rate parameter (i.e., the second-derivative of the phase) can be obtained by:

$$\phi^{(2)}(t) \approx \frac{\phi(t+nT) - 2\phi(t) + \phi(t-nT)}{2(nT)^2}. \quad (5)$$

This approximate formula corresponds to the local auto-correlation function $f(t+nT)f^{*2}(t)f(t-nT)$. Since $f^{*2}(t)$ does not depend on nT , the CPF was proposed for the chirp-rate estimation:

$$\begin{aligned}C_h(t, \Omega) &= \sum_{n=-\infty}^{\infty} w_h(nT) \times \\ &\quad f(t+nT)f(t-nT)\exp(-j\Omega(nT)^2).\end{aligned}\quad (6)$$

where Ω denotes chirp-rate index. The rectangular window function (finite number of

samples) is inherently assumed in the original O'Shea estimator. Here, in our derivations of the adaptive chirp-rate estimator, we will assume that a general window function is used. The CPF-based nonparametric chirp-rate estimation can be performed as:

$$\hat{\Omega}_h(t) = \arg \max_{\Omega} |C_h(t, \Omega)|^2. \quad (7)$$

In this manner the non-linearity of the chirp-rate estimation is kept to the same order as in the WD case, i.e., the second order non-linearity. It results in high accuracy approaching the Cramer-Rao lower bound (CRLB) for a wide range of the SNR for Gaussian noise environment [10], [11], [13].

However, non-polynomial phase signal or high-order polynomial phase signal this estimator is biased, and the performance degrades. To relax the application range of the CPF-based chirp-rate estimator, in this following, an CPF-based algorithm with adaptive window width is proposed. Specifically, the window width is adaptively determined by using the ICI algorithm.

III. ASYMPTOTIC BIAS AND VARIANCE

The chirp-rate is estimated by using the position of the peaks in the magnitude-squared CPF. The CPF is ideally concentrated on the chirp-rate for signals, when the fourth and other higher-order phase derivatives are equal to zero. However, for signals with these derivatives being different from zero, this is not the case. Higher order derivatives produce bias in the chirp-rate estimation. The asymptotic expression for the bias, derived in the Appendix, is:

$$\text{bias}\{\hat{\Omega}_h(t)\} = E\{\Delta\Omega_h(t)\} \simeq \phi^{(4)}(t)w_b h^2, \quad (8)$$

where w_b is a constant dependent on the selected window type only, while $\phi^{(4)}(t)$ is the fourth derivative of the signal phase. Assume that the signal corrupted by the additive white Gaussian noise $\nu(t)$ with:

- mutually independent real and imaginary parts,
- zero-mean $E\{\nu(t)\} = 0$ and
- covariance $E\{\nu(t')\nu^*(t'')\} = \sigma^2\delta(t' - t'')$, where σ^2 is variance while $\delta(t)$ is the Dirac

delta function defined $\delta(t) = 1$ for $t = 0$ and $\delta(t) = 0$ elsewhere.

Then, the asymptotic expression for variance of the chirp-rate estimator (7), for relatively high SNR, exhibits:

$$\text{var}\{\hat{\Omega}_h(t)\} \simeq \frac{\sigma^2}{A^2} h^{-5} w_v, \quad (9)$$

where w_v depends on the selected window type only (see Appendix). Obviously, the bias increases with the increase of the window width, while the variance decreases at the same time. The MSE of the estimator is

$$\begin{aligned} & \text{MSE}\{\hat{\Omega}_h(t)\} \\ &= \text{bias}^2\{\hat{\Omega}_h(t)\} + \text{var}\{\hat{\Omega}_h(t)\} \\ &= [\phi^{(4)}(t)]^2 w_b^2 h^4 + \frac{\sigma^2}{A^2} h^{-5} w_v. \end{aligned} \quad (10)$$

From (10), by minimizing the MSE with respect to h , we get

$$h_{opt}(t) = \sqrt[9]{\frac{5 \frac{\sigma^2}{A^2} w_h}{4[\phi^{(4)}(t)]^2 w_b^2}}. \quad (11)$$

Since the fourth order derivative of the signal phase is not known in advance, we cannot determine the optimal window length $h_{opt}(t)$ in practice. In this paper, an algorithm that can produce adaptive window width, close to the optimal one, is proposed without knowing phase derivatives in advance. The ICI algorithm [2]-[7] is developed for similar problems with a trade-off in parameter selection between the bias and variance. The ICI-based algorithm for the second order derivative estimation is given in the next section.

IV. INTERSECTION CONFIDENCE INTERVAL ALGORITHM

Here, we will briefly describe the ICI algorithm for achieving the trade-off between influence of the higher-order derivatives (bias) and noise (variance). Consider the set of increasing window widths $H = \{h_1, h_2, \dots, h_Q\}$, $h_i < h_{i+1}$. These windows are selected in such a manner that $h_i \approx a^{i-1} h_1$, $a > 1$. It is assumed that the optimal window $h_{opt}(t)$, for a given instant, is close to a value from

the considered set. Chirp-rate estimates corresponding to all windows from H are $\hat{\Omega}_{h_i}(t)$, $i = 1, 2, \dots, Q$. They are obtained as:

$$\hat{\Omega}_{h_i}(t) = \arg \max_{\Omega} |C_{h_i}(t, \Omega)|^2, \quad (12)$$

where $C_{h_i}(t, \Omega)$ is the CPF calculated with window $w_{h_i}(t)$ of the width h_i , $w_{h_i}(t) \neq 0$ for $|t| \leq h_i/2$. Around any estimate we can create a confidence interval $[\hat{\Omega}_{h_i}(t) - \kappa\sigma(h_i), \hat{\Omega}_{h_i}(t) + \kappa\sigma(h_i)]$, where κ is the parameter that controls probability that exact chirp-rate parameter belongs to the interval, while $\sigma(h_i) = \frac{\sigma}{A} h_i^{-5/2} \sqrt{w_v}$ (21). For Gaussian variable we know that exact value of the parameter belongs to the interval with probability $P(\kappa)$ (for example, $P(2) = 0.95$ and $P(3) = 0.997$).

According to [7], the optimal window is close to the widest one where the confidence intervals, created with two neighboring windows from set H , still intersects. This can be written as:

$$|\hat{\Omega}_{h_i}(t) - \hat{\Omega}_{h_{i-1}}(t)| \leq \kappa(\sigma(h_i) + \sigma(h_{i-1})). \quad (13)$$

It is required that this relationship holds also for all narrower windows:

$$\begin{aligned} & |\hat{\Omega}_{h_j}(t) - \hat{\Omega}_{h_{j-1}}(t)| \leq \kappa(\sigma(h_j) + \sigma(h_{j-1})), \\ & j \leq i. \end{aligned} \quad (14)$$

Then we can adopt that the optimal window estimate for the considered instant is $\hat{h}_{opt}(t) = h_i$ or $\hat{h}_{opt}(t) = h_{i-1}$.

As it is shown in [2], selection of particular window depends on bias and variance (in fact on powers of parameter of interest h^n and h^{-m}) in considered application. Namely, in our application $\text{bias}^2\{\hat{\Omega}_h(t)\} \propto h^4$ while $\text{var}\{\hat{\Omega}_h(t)\} \propto h^{-5}$. Then, according to [2], it is better to take previous window $\hat{h}_{opt}(t) = h_{i-1}$ as the optimal estimate since the next window can already have large bias. The algorithm accuracy depends on the proper selection of parameter κ . This selection is discussed in details in [2]. It can be assumed that algorithm for relatively wide region of $\kappa \in [2, 5]$ produces results of the same order of accuracy. The cross-validation algorithm [4] or results from analysis given in [2] can be employed in the

case where precise selection of this parameter is required. In our simulations, $\kappa = 3$ is used.

The remaining question in the algorithm is how to estimate $\sigma(h_i)$ since the signal amplitude and noise variance (A and σ) are not known in advance. There are several approaches in the literature, but here we will use a simple and very accurate technique from [30]. Namely, amplitude can be estimated as:

$$\hat{A}^2 = \sqrt{|2M_2^2 - M_4|} \quad (15)$$

where

$$M_i = \frac{1}{N} \sum x^i(n), \quad (16)$$

where N is number of signal samples, while the variance can be estimated as:

$$\hat{\sigma}^2 = |M_2 - \hat{A}^2|. \quad (17)$$

V. NUMERICAL EXAMPLES

We considered two test signals:

$$f_1(t) = \begin{cases} \exp(j12\pi t^2) & t \geq 0 \\ \exp(-j12\pi t^2) & t < 0 \end{cases} \quad (18)$$

and

$$f_2(t) = \exp(j8\pi t^4). \quad (19)$$

The exact chirp-rates for these two signals are $\Omega_1(t) = 24\pi\text{sign}(t)$ and $\Omega_2(t) = 96\pi t^2$. Signal is considered within interval $t \in [-1/2, 1/2]$ with sampling rate $T = 1/257$. Set of used window widths is $h_i = N_i T$, where $N_i = a^{i-1} N_1$ and $a = \sqrt{2}$ and $N_1 = 5$. We always set the closest possible window from the set with odd number of samples in the interval. Total number of windows in the set is 13. Figure 1 depicts the MSE of the obtained chirp-rate estimators for: $\sigma = 0.06$ (first row, $SNR = 24\text{dB}$), $\sigma = 0.09$ (second row, $SNR = 21\text{dB}$) and $\sigma = 0.12$ (third row, $SNR = 18\text{dB}$). The left column is given for the first test signal (18) while the right column represents results for the second test signal (19). Results are obtained with the Monte Carlo simulation with 100 trials. Thin line marks results obtained with the windows of the fixed width, while thick line represents results achieved with the proposed algorithm. It

can be seen that the proposed algorithm gives more accurate results than almost all windows with fixed width. It may happen that some of windows with fixed width outperform our algorithm, but it should be kept in mind that the best window is not known in advance. For example, it can be seen that the best fixed window width for the first test signal and $\sigma = 0.06$ (Fig. 1a) is about $N = 20$ samples, for the second signal and the same noise it is about $N = 50$ samples (Fig. 1b), while for the first signal and $\sigma = 0.12$ (Fig. 1e) it is about $N = 70$ samples.

Illustration of the adaptive CPF for the chirp-rate estimation for the first test signal embedded in the noise with $\sigma = 0.09$ is depicted in Figure 2. Figs. 2a-f represent the result obtained with fixed window widths ($N = 9, N = 17, N = 33, N = 65, N = 129,$ and $N = 257$). Results obtained with the proposed algorithm are presented in Fig. 2g. Bias in the region close to the abrupt change can be observed. It is caused by the fact that we need a narrow window in this region and that this window produces estimate highly corrupted by noise (see Fig. 2a). Fig. 2h depicts the adaptive window width.

Results achieved with the second test signal for $\sigma = 0.09$ are depicted in Figure 3. Here, the fourth order derivative of the signal phase is constant and we can expect that the optimal window width is constant. High noise influence can be observed for small window widths (Fig. 3b, c, $N = 9$ and $N = 17$) while, at the same time, the bias can be seen for wide window (Fig. 3f, $N = 257$). The chirp-rate estimate and corresponding adaptive window width are depicted in Figs. 3g, h. It can be seen that the proposed algorithm gives adaptive window width close to constant as it was expected.

VI. CONCLUSION

An adaptive chirp-rate estimator is introduced for a general signal model. It is based on the confidence intervals-rule. Selection of the algorithm parameters is discussed. The proposed algorithm is tested on two characteristic test signals. The obtained results are good, close to the optimal one that can be achieved

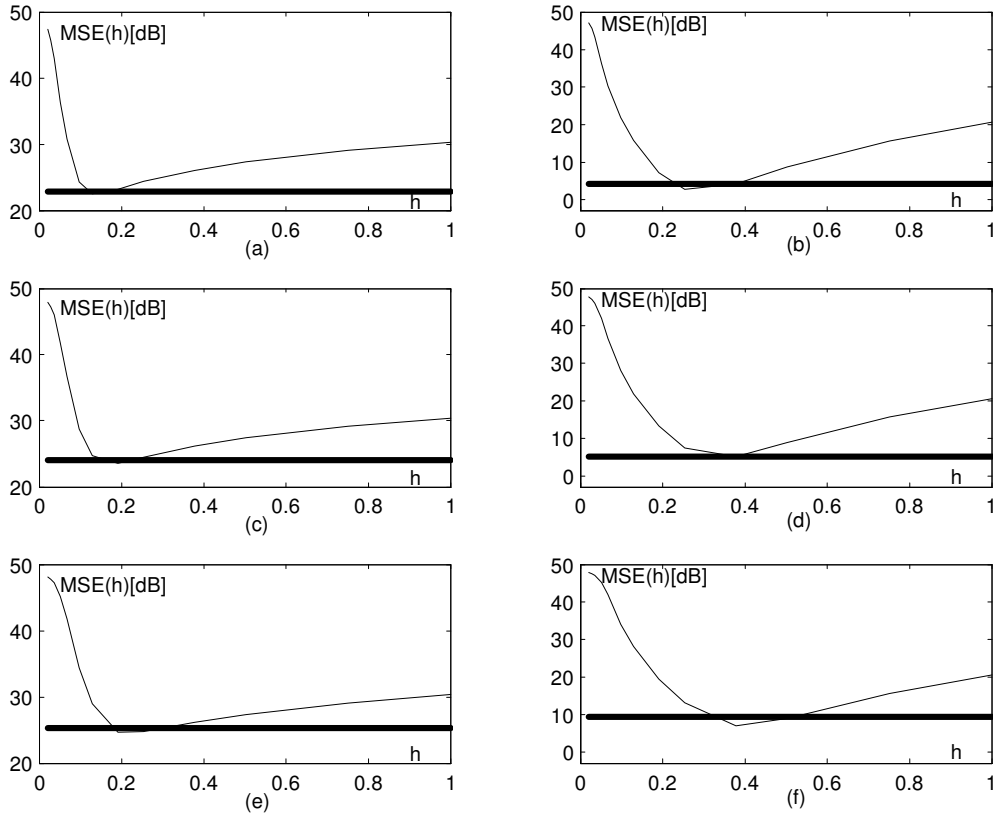


Fig. 1. MSE for the chirp-rate estimation: (a) Signal 1, $\sigma = 0.06$; (b) Signal 2, $\sigma = 0.06$; (c) Signal 1, $\sigma = 0.09$; (d) Signal 2, $\sigma = 0.09$; (e) Signal 1, $\sigma = 0.12$; (f) Signal 2, $\sigma = 0.12$. Thin line - fixed window estimator; Thick line - adaptive window width.

with the CPF function.

APPENDIX

I. ASYMPTOTIC BIAS AND VARIANCE

Our observation is modeled as $x(t) = f(t) + \nu(t)$ where $f(t) = A \exp(j\phi(t))$, while $\nu(t)$ is Gaussian noise with mutually independent real and imaginary parts, with zero-mean $E\{\nu(t)\} = 0$ and $E\{\nu(t')\nu^*(t'')\} = \sigma^2\delta(t' - t'')$. Chirp-rate is estimated by using position of the CPF maximum. The CPF is ideally concentrated on the chirp-rate for noiseless signals when $\phi^{(k)}(t) = 0$ for $k > 3$. Introduce the following notation $F_h(t, \Omega) = |C_h(t, \Omega)|^2$ for squared-magnitude of the CPF. Here, index h denotes width of the used even window function, $w_h(t) \neq 0$ for $|t| \leq h/2$, $w_h(t) = w_h(-t)$. Two main sources of errors in the CPF are: 1) errors caused by non-zero higher-order deriv-

atives of the signal phase (contributing to the bias); 2) errors caused by the noise (contributing to the variance). For the sake of brevity, here we will give the main steps of the derivations. According to [3], the bias of the chirp-rate estimator can be expressed as:

$$E\{\Delta\Omega_h(t)\} = \text{bias}\{\hat{\Omega}_h(t)\} = -\frac{\frac{\partial F_h(t, \Omega)}{\partial \Omega} \Big|_{0\delta_{\Delta\Omega}}}{\frac{\partial^2 F_h(t, \Omega)}{\partial \Omega^2} \Big|_0}, \tag{20}$$

while the variance is

$$\text{var}\{\hat{\Omega}_h(t)\} = \frac{E\left\{\left[\frac{\partial F_h(t, \Omega)}{\partial \Omega} \Big|_{0\delta_\nu}\right]^2\right\}}{\left[\frac{\partial^2 F_h(t, \Omega)}{\partial \Omega^2} \Big|_0\right]^2}, \tag{21}$$

where:

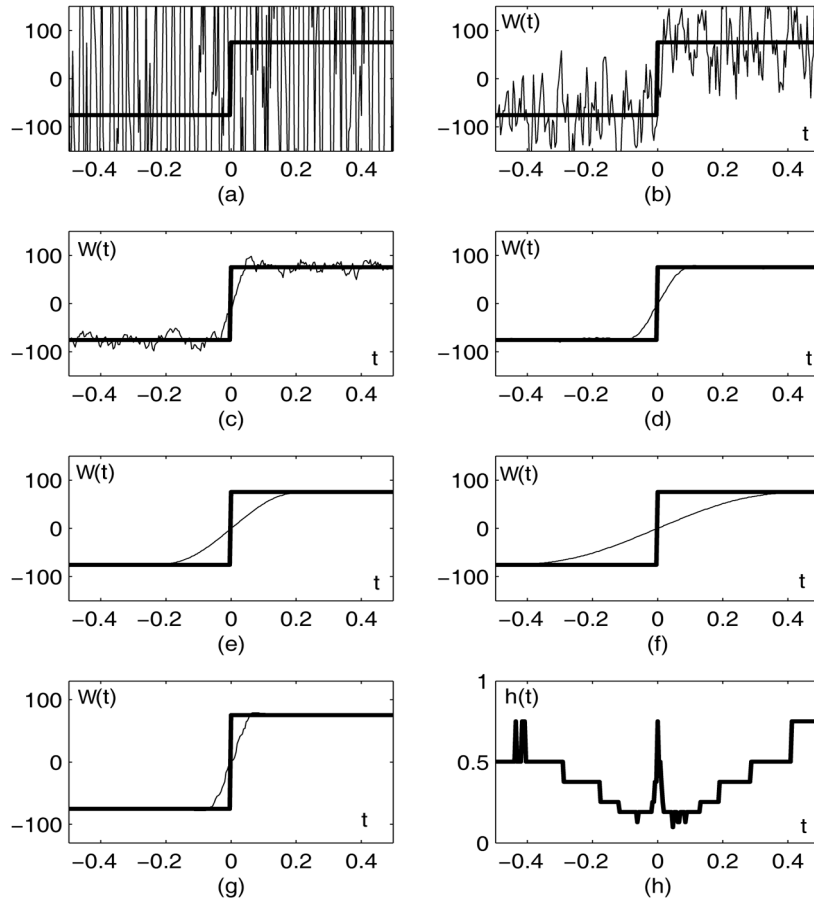


Fig. 2. Chirp-rate estimation for test signal 1: (a) Fixed window $N = 9$ samples ($h = 9/257$); (b) Fixed window $N = 17$ samples ($h = 17/257$); (c) Fixed window $N = 33$ samples ($h = 33/257$); (d) Fixed window $N = 65$ samples ($h = 65/257$); (e) Fixed window $N = 129$ samples ($h = 129/257$); (f) Fixed window $N = 257$ samples ($h = 1$); (g) Estimator with adaptive window width; (h) Adaptive window width.

- $\partial^2 F_h(t, \Omega) / \partial \Omega^2|_0$ is evaluated at the position of the true chirp-rate, with the assumption that the signal has all phase derivatives higher than 2 equal to zero and that there is no noise;
- $\partial F_h(t, \Omega) / \partial \Omega|_{0\delta_{\Delta\Omega}}$ is evaluated at the position of true chirp-rate with assumption that estimation error is caused only by higher-order derivatives of the signal phase (noise-free assumption);
- $\partial F_h(t, \Omega) / \partial \Omega|_{0\delta_{\nu}}$ is evaluated at the position of the true chirp-rate with the assumption that there is no higher order phase derivatives, i.e., noise only influenced error.

Then three intermediate quantities $\frac{\partial^2 F_h(t, \Omega)}{\partial \Omega^2}|_0$, $\frac{\partial F_h(t, \Omega)}{\partial \Omega}|_{0\delta_{\Delta\Omega}}$, and $E \left\{ \left[\frac{\partial F_h(t, \Omega)}{\partial \Omega}|_{0\delta_{\nu}} \right]^2 \right\}$ are needed to determine asymptotic bias and variance. Calculations of these quantities are shown below.

A. Determination of $\partial^2 F_h(t, \Omega) / \partial \Omega^2|_0$

Determination of $\partial^2 F_h(t, \Omega) / \partial \Omega^2|_0$ is performed on true chirp-rate, i.e., $\Omega = \phi^{(2)}(t)$ under assumption that there is noise and higher order terms in the signal phase. Then the CPF exhibits:

$$C_h(t, \Omega) = \exp(j^2\phi(t)) \sum_{n=-\infty}^{\infty} w_h(nT)$$

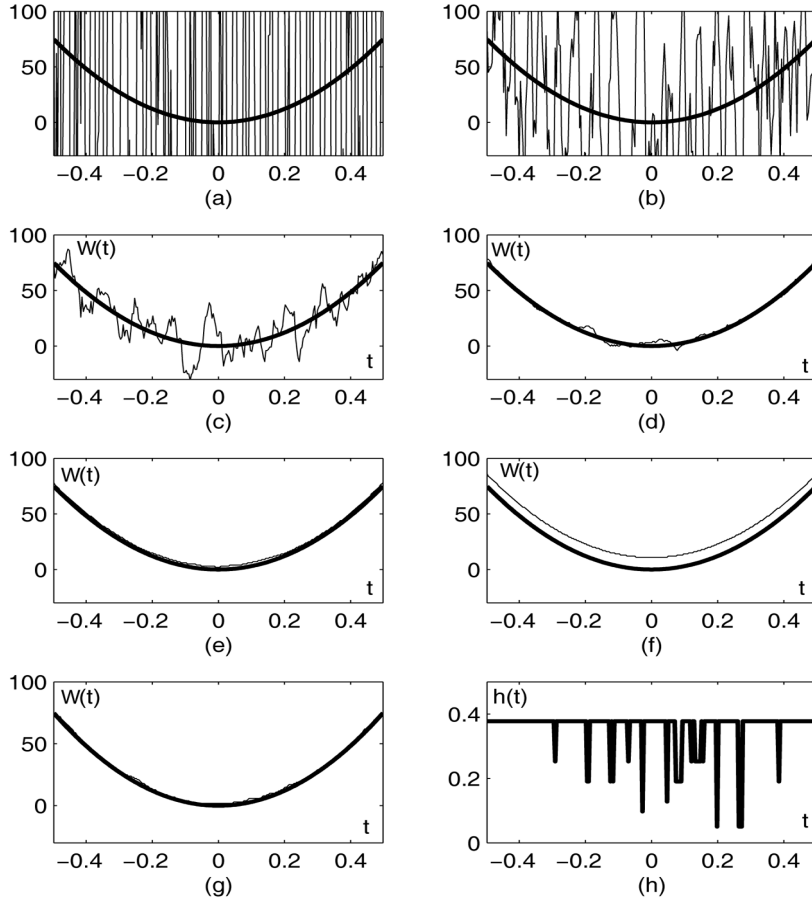


Fig. 3. Chirp-rate estimation for test signal 2: (a) Fixed window $N = 9$ samples ($h = 9/257$); (b) Fixed window $N = 17$ samples ($h = 17/257$); (c) Fixed window $N = 33$ samples ($h = 33/257$); (d) Fixed window $N = 65$ samples ($h = 65/257$); (e) Fixed window $N = 129$ samples ($h = 129/257$); (f) Fixed window $N = 257$ samples ($h = 1$); (g) Estimator with adaptive window width; (h) Adaptive window width.

$$\times A^2 \exp(j\phi^{(2)}(t)(nT)^2) \exp(-j\Omega(nT)^2). \quad (22)$$

Value of $F_h(t, \Omega) = |C_h(t, \Omega)|^2$ is:

$$F_h(t, \Omega) = A^4 \sum_{n_1=-\infty}^{\infty} \sum_{n_2=-\infty}^{\infty} w_h(n_1T) w_h^*(n_2T) \times \exp(j\phi^{(2)}(t)(n_1T)^2 - j\phi^{(2)}(t)(n_2T)^2) \times \exp(-j\Omega(n_1T)^2 + j\Omega(n_2T)^2) \quad (23)$$

The second partial derivative $\partial^2 F_h(t, \Omega) / \partial \Omega^2|_0$, evaluated for $\Omega = \phi^{(2)}(t)$, is:

$$\frac{\partial^2 F_h(t, \Omega)}{\partial \Omega^2} \Big|_0 = - \sum_{n_1} \sum_{n_2} A^4 w_h(n_1T)$$

$$\begin{aligned} & \times w_h^*(n_2T) ((n_1T)^2 - (n_2T)^2)^2 \\ & = -2A^4 \sum_{n_1} \sum_{n_2} w_h(n_1T) w_h(n_2T) \\ & \quad \times [(n_1T)^4 - (n_1T)^2(n_2T)^2] \\ & = 2A^4 h^4 [F_2^2 - F_4 F_0], \end{aligned} \quad (24)$$

where (see Appendix of [3])

$$F_k = \int_{-1/2}^{1/2} w(t) t^k dt. \quad (25)$$

B. Determination of $\partial F_h(t, \Omega) / \partial \Omega|_{0\delta_{\Delta\Omega}}$

Assumptions in the evaluation of the second term $\partial F_h(t, \Omega) / \partial \Omega|_{0\delta_{\Delta\Omega}}$ are similar like for the

first terms, except the influence of the higher-order phase terms that now is not neglected:

$$\begin{aligned} & \frac{\partial F_h(t, \Omega)}{\partial \Omega} \Big|_{0\delta_{\Delta\Omega}} = \\ & A^4 \sum_{n_1} \sum_{n_2} w_h(n_1 T) w_h^*(n_2 T) \\ & \quad \times (-j((n_1 T)^2 - (n_2 T)^2)) \\ & \times \exp\left(2j \sum_{k=2}^{\infty} \phi^{(2k)}(t) \frac{(n_1 T)^{2k} - (n_2 T)^{2k}}{(2k)!}\right). \quad (26) \end{aligned}$$

For simplicity, all higher-order derivatives, except the fourth order are removed, i.e., $|\phi^{(4)}(t)| \gg |\phi^{(2k)}(t)|$ for $k > 2$:

$$\begin{aligned} & \frac{\partial F_h(t, \Omega)}{\partial \Omega} \Big|_{0\delta_{\Delta\Omega}} = A^4 \sum_{n_1} \sum_{n_2} w_h(n_1 T) \\ & \quad \times w_h^*(n_2 T) (-j((n_1 T)^2 - (n_2 T)^2)) \\ & \quad \times \exp\left(j \phi^{(4)}(t) \frac{(n_1 T)^4 - (n_2 T)^4}{12}\right). \quad (27) \end{aligned}$$

Under the assumption that argument of exponential function $\phi^{(4)}(t) \frac{(n_1 T)^4 - (n_2 T)^4}{12}$ is relatively small, we can write

$$\begin{aligned} & \exp\left(j \phi^{(4)}(t) \frac{(n_1 T)^4 - (n_2 T)^4}{12}\right) \\ & \approx 1 + j \phi^{(4)}(t) \frac{(n_1 T)^4 - (n_2 T)^4}{12}. \quad (28) \end{aligned}$$

Finally, we get:

$$\begin{aligned} & \frac{\partial F_h(t, \Omega)}{\partial \Omega} \Big|_{0\delta_{\Delta\Omega}} \\ & = \phi^{(4)}(t) \sum_{n_1} \sum_{n_2} A^4 w_h(n_1 T) w_h^*(n_2 T) \\ & \quad \times ((n_1 T)^2 - (n_2 T)^2)((n_1 T)^4 - (n_2 T)^4) \\ & = 2A^4 \phi^{(4)}(t) h^6 [F_6 F_0 - F_2 F_4]. \quad (29) \end{aligned}$$

C. Determination of $E \left\{ \left[\frac{\partial F_h(t, \Omega)}{\partial \Omega} \Big|_{0\delta_{\Delta\Omega}} \right]^2 \right\}$

In the evaluation of $E \left\{ \left[\frac{\partial F_h(t, \Omega)}{\partial \Omega} \Big|_{0\delta_{\Delta\Omega}} \right]^2 \right\}$ higher-order phase terms are removed while now we consider the influence of the additive Gaussian noise. Then, the term required for determination of the variance is given as:

$$E \left\{ \left[\frac{\partial F_h(t, \Omega)}{\partial \Omega} \Big|_{0\delta_{\Delta\Omega}} \right]^2 \right\}$$

$$\begin{aligned} & = \sum_{n_1} \sum_{n_2} \sum_{n_3} \sum_{n_4} w_h(n_1 T) \\ & \quad \times w_h(n_2 T) w_h(n_3 T) w_h(n_4 T) \\ & \quad \times E \{ x(t+n_1 T) x(t-n_1 T) x^*(t+n_2 T) x^*(t-n_2 T) \\ & \quad \times x^*(t+n_3 T) x^*(t-n_3 T) x(t+n_4 T) x(t-n_4 T) \} \\ & \quad \times ((n_1 T)^2 - (n_2 T)^2)((n_3 T)^2 - (n_4 T)^2) \\ & \quad \times \exp(-j\Omega(n_1 T)^2 + j\Omega(n_2 T)^2 + j\Omega(n_3 T)^2 - \Omega(n_4 T)^2). \quad (30) \end{aligned}$$

Determination of

$$\begin{aligned} & E \{ x(t+n_1 T) x(t-n_1 T) x^*(t+n_2 T) \\ & \quad \times x^*(t-n_2 T) x^*(t+n_3 T) x^*(t-n_3 T) \\ & \quad \times x(t+n_4 T) x(t-n_4 T) \} \quad (31) \end{aligned}$$

is a rather tedious job. By assuming high SNR, i.e., $A^2/\sigma^2 \gg 1$, the above equation can be approximated by using only terms with two noise factors. Then, from all possible 128 combinations of signal and noise we can select just those where we have 2 noise terms and 6 signal terms. Namely, combinations with 1 and 3 noise terms give expectation equal to zero, while we can assume that combinations with 4 and more noise terms due to introduced high SNR assumption are much smaller than the expectation of combinations with 2 noise terms. There are 28 combinations in total, with 2 noise terms. Fortunately, a high number of them have zero expectation. Namely, for the used noise model (complex Gaussian noise with independent real and imaginary parts) it holds $E\{\nu(t_1)\nu(t_2)\} = E\{\nu^*(t_1)\nu^*(t_2)\} = 0$. This eliminates 12 combinations from (31). Furthermore, combinations $E\{\nu(t \pm n_1 T)\nu^*(t \pm n_2 T)\} = \sigma^2 \delta(n_1 \pm n_2)$ and combinations $E\{\nu^*(t \pm n_3 T)\nu(t \pm n_4 T)\} = \sigma^2 \delta(n_3 \pm n_4)$ will also produce a zero-mean, since they cause $(n_1 T)^2 - (n_2 T)^2 = 0$ or $(n_3 T)^2 - (n_4 T)^2 = 0$ in (30). This eliminates next 8 combinations. Only 8 remaining combinations: $E\{\nu(t \pm n_1 T)\nu^*(t \pm n_3 T)\} = \sigma^2 \delta(n_1 \pm n_3)$ and $E\{\nu^*(t \pm n_2 T)\nu(t \pm n_4 T)\} = \sigma^2 \delta(n_2 \pm n_4)$ give results of interest. We will consider just one of these 8 combinations, since all others produce the same result. Here, we will consider situation where the first term

$x(t + n_1T)$ and the fifth $x^*(t + n_3T)$ are noisy terms while others are signal terms:

$$\begin{aligned}
& \sum_{n_1} \sum_{n_2} \sum_{n_3} \sum_{n_4} w_h(n_1T)w_h(n_2T)w_h(n_3T) \\
& \times w_h(n_4T)\sigma^2\delta(n_1 - n_3)f(t - n_1T)f^*(t + n_2T) \\
& \quad \times f^*(t - n_2T)f^*(t + n_3T)f^*(t - n_3T) \\
& \times f(t + n_4T)f(t - n_4T)\{(n_1T)^2 - (n_2T)^2\} \\
& \quad \times \{(n_3T)^2 - (n_4T)^2\} \\
& \times e^{(-j\Omega(n_1T)^2 + j\Omega(n_2T)^2 + j\Omega(n_3T)^2 - \Omega(n_4T)^2)} \\
& = \sum_{n_1} \sum_{n_2} \sum_{n_4} \sigma^2 |f(t - n_1T)|^2 w_h^2(n_1T) \\
& \times w_h(n_2T)w_h(n_4T)f^*(t + n_2T)f^*(t - n_2T) \\
& \times f(t + n_4T)f(t - n_4T)\{(n_1T)^2 - (n_2T)^2\} \\
& \quad \times \{(n_1T)^2 - (n_4T)^2\} e^{(j\Omega(n_2T)^2 - \Omega(n_4T)^2)} \\
& = \sigma^2 A^6 \sum_{n_1} \sum_{n_2} \sum_{n_4} w_h^2(n_1T)w_h(n_2T) \\
& \times w_h(n_4T)\{(n_1T)^2 - (n_2T)^2\}\{(n_1T)^2 - (n_4T)^2\} \\
& = \sigma^2 A^6 h^3 [E_4 F_0^2 - 2E_2 F_2 F_0 + E_0 F_2^2], \quad (32)
\end{aligned}$$

where E_k is calculated according to [3]

$$E_k = \frac{1}{T} \int_{-1/2}^{1/2} w^2(t) t^k dt.$$

The same results as (32) can be obtained for the other seven terms, so we have

$$\begin{aligned}
& E \left\{ \left[\frac{\partial F_h(t, \Omega)}{\partial \Omega} \Big|_{0\delta_\nu} \right]^2 \right\} \\
& = 8\sigma^2 A^6 h^3 [E_4 F_0^2 - 2E_2 F_2 F_0 + E_0 F_2^2]. \quad (33)
\end{aligned}$$

Substituting (24), (29), and (33) in (20) and (21) we are getting expressions for the bias and variance (8) and (9).

ACKNOWLEDGEMENT

The work of Igor Djurović is realized at the INP Grenoble, France, and supported by the CNRS, under contract No. 18008901300387. The work of Pu Wang was supported in part by the National Natural Science Foundation of China under Grant 60802062.

REFERENCES

- [1] B. Boashash, "Estimating and interpreting the instantaneous frequency of a signal - Part I," *Proc. IEEE*, Vol. 80, No.4, Apr. 1992, pp. 521-538.
- [2] L.J. Stanković, "Performance analysis of the adaptive algorithm for bias-to-variance tradeoff," *IEEE Trans. Sig. Proc.*, Vol. 52, No. 5, May 2004, pp. 1228-1234.
- [3] V. Katkovnik and L.J. Stanković, "Instantaneous frequency estimation using the Wigner distribution with varying and data driven window length," *IEEE Trans. Sig. Proc.*, Vol. 46, No.9, Sept. 1998, pp. 2315-2325.
- [4] V. Katkovnik and L.J. Stanković, "Periodogram with varying and data-driven window length," *Signal Process.*, Vol. 67, No. 3, pp. 345-358, 1998.
- [5] L.J. Stanković and V. Katkovnik, "Algorithm for the instantaneous frequency estimation using time-frequency distributions with variable window width," *IEEE Signal Processing Lett.*, Vol. 5, pp. 224-228, Sept. 1998.
- [6] L.J. Stanković and V. Katkovnik, "Instantaneous frequency estimation using higher order distributions with adaptive order and window length," *IEEE Trans. Inform. Theory*, Vol. 46, pp. 302-311, Jan. 2000.
- [7] L.J. Stanković, "Adaptive instantaneous frequency estimation using TFDs," in *Time-Frequency Signal Analysis and Processing*, B. Boashash, Ed. New York: Elsevier, 2003.
- [8] I. Djurović, T. Thayaparan, L.J. Stanković, "SAR imaging of moving targets using polynomial FT", *IET Proc. Sig. Proc.*, Vol. 2, No. 3, pp.237-246, 2008.
- [9] I. Djurović, T. Thayaparan, L.J. Stanković, "Adaptive local polynomial Fourier transform in ISAR", *Journal of Applied Signal Processing*, Vol. 2006, Article ID 36093, 2006.
- [10] P. O'Shea: "A fast algorithm for estimating the parameters of a quadratic FM signal," *IEEE Tran. Sig. Proc.*, Vol. 52, No. 2, Feb. 2004, pp. 385-393.
- [11] M. Farquharson and P. O'Shea, "Extending the performance of the cubic phase function algorithm," *IEEE Tran. Sig. Proc.*, Vol. 55, No. 10, Oct. 2007, pp. 4767-4774.
- [12] M. Farquharson, P. O'Shea and G. Ledwich, "A computationally efficient technique for estimating the parameters of polynomial phase signals from noisy observations," *IEEE Tran. Sig. Proc.*, Vol. 53, No. 8, Aug. 2005, pp. 3337-3342.
- [13] P. O'Shea, "A new technique for instantaneous frequency rate estimation," *IEEE Sig. Proc. Lett.*, Vol. 9, No. 8, Aug. 2002, pp. 251-252.
- [14] P. Wang, I. Djurović and J. Yang, "Instantaneous frequency rate estimation based on robust cubic phase function," in *Proc. of IEEE ICASSP'06*, Toulouse, France, Sept. 2006.
- [15] V. Katkovnik, K. Egiazarian, and J. Astola, "Application of the ICI principle to window size adaptive median filtering," *Signal Process.*, Vol. 83, No. 1, pp. 251-257, Feb. 2003.
- [16] B. Krstajić, L.J. Stanković, and Z. Uskoković, "An approach to variable step-size LMS algorithm," *IEE Electron. Lett.*, Vol. 38, No. 16, pp. 927-928, Aug. 2002.
- [17] J. Astola, K. Egiazarian, and V. Katkovnik, "Adaptive window size image denoising based on

- ICI rule,” in *Proc. Int. Conf. Acoust., Speech, Signal Process.*, Vol. 3, 2001, pp. 1869–1872.
- [18] I. Djurović, L.J. Stanković, “Modification of the ICI rule based IF estimator for high Noise environments”, *IEEE Trans. Signal Processing*, Vol. 52, No.9, 2004, pp. 2655-2661.
- [19] B. Barkat, “Instantaneous frequency estimation of nonlinear frequency-modulated signals in the presence of multiplicative and additive noise,” *IEEE Trans. Signal Processing*, Vol. 49, pp. 2214–2222, Oct 2001.
- [20] Z. M. Hussain and B. Boashash, “Adaptive instantaneous frequency estimation of multicomponent FM signals using quadratic time-frequency distributions,” *IEEE Trans. Signal Processing*, Vol. 50, pp. 1676–1866, Aug. 2002.
- [21] T. Abotzoglou, “Fast maximum likelihood joint estimation of frequency and frequency rate,” *IEEE Trans. on Aerosp. Electron. Syst.*, Vol. 22, pp. 708–715, Nov. 1986.
- [22] P. M. Djuric and S. Kay, “Parameter estimation of chirp signals,” *IEEE Trans. Sig. Proc.*, vol. 38, no. 12, pp. 2118–2126, Dec. 1990.
- [23] S. Peleg and B. Porat, “Linear FM signal parameter estimation from discrete-time observations,” *IEEE Trans. Aerosp. Electron. Syst.*, Vol. 27, No. 4, pp. 607–614, Jul. 1991.
- [24] J. C. Wood and D. T. Barry, “Radon transformation of time-frequency distributions for analysis of multicomponent signals,” *IEEE Trans. Sig. Proc.*, Vol. 42, No. 11, pp. 3166–3177, Nov. 1994.
- [25] S. Barbarossa, “Analysis of multicomponent LFM signals by a combined Wigner-Hough transform,” *IEEE Trans. Sig. Proc.*, Vol. 43, No. 6, pp. 1511–1515, Jun, 1995.
- [26] B. Friedlander and J. M. Francos, “Estimation of amplitude and phase parameters of multicomponent signals,” *IEEE Trans. Sig. Proc.*, Vol. 43, No. 4, pp. 917–926, Apr. 1995.
- [27] S. Peleg and B. Friedlander, “Multicomponent signals analysis using the polynomial-phase transform,” *IEEE Trans. Aerosp. Electron. Syst.*, Vol. 32, No. 1, pp. 378–387, Jan. 1996.
- [28] S. Barbarossa, A. Scaglione, and G. Giannakis, “Product high-order ambiguity function for multicomponent polynomial phase signal modeling,” *IEEE Trans. Sig. Proc.*, Vol. 46, No. 3, pp. 691–708, Mar. 1998.
- [29] L. Cirillo, A. Zoubir, and M. Amin, “Parameter estimation for locally linear FM signals using a time-frequency Hough transform,” *IEEE Trans. Sig. Proc.*, Vol. 56, No. 9, Sept. 2008, pp. 4162–4175.
- [30] S.-C. Sekhar, T.V. Creenivas, “Signal to noise ratio estimation using higher order moments”, *Signal Processing*, Vol. 86, 2006., pp 716-732.